# Storage and distribution of organic carbon in cave sediments: examples from two caves in the northern karst region of Puerto Rico

**Autum R Downey**
West Virginia University Eberly College of Arts and Sciences
**Jill L Riddell**
West Virginia University Eberly College of Arts and Sciences
**Ingrid Y Padilla**
University of Puerto Rico Mayaguez: Recinto Universitario de Mayaguez Universidad de Puerto Rico
**Dorothy J Vesper** ( djvesper@mail.wvu.edu )
West Virginia University https://orcid.org/0000-0002-2096-7548

**Research Article**

**Keywords:** karst, cave, sediment, organic carbon, TOC

**Posted Date:** April 14th, 2022

**DOI:** https://doi.org/10.21203/rs.3.rs-1459657/v1



**Version of Record:** A version of this preprint was published at Environmental Earth Sciences on December 29th, 2022. See the published version at https://doi.org/10.1007/s12665-022-10720-2.

# Abstract

The clastic sediments that accumulate in cave settings can be an important storage reservoir for organic carbon, affect contaminant fate and transport, and contribute to ecosystem processes. This study reports on grain size, total organic carbon (TOC) concentrations, and total organic carbon:total organic nitrogen (TOC:TON) ratios measured in sediments from two caves in Puerto Rico. El Tallonal Cave (TAL) is a small cave with a flowing stream; the sediments from TAL were collected from a deposit that is being actively eroded. Cueva Cave (CAM) is an upper level of the Río Camuy Cave System; the sediments from CAM were newly deposited by an internal river that rose in response to Hurricane Maria. Sediments collected from both caves were poorly sorted and contained no apparent stratigraphic correlation. CAM sediments contained a larger range in TOC concentrations but were overall lower than TOC in the TAL sediments. In TAL, the TOC concentrations were higher in sediments collected from below the usual water level. TOC:TON ratios from sediments at both caves were highly variable, highlighting the heterogeneous deposition and storage of organic matter. Despite the observed variation, TOC concentrations in both cave systems cause retardation of organic contaminants by up to two orders-of-magnitude, implying that deposited sediments influence the fate of organic contaminants in the groundwater; therefore, cave sediments could facilitate long term storage of organic carbon and associated contaminants.


# Introduction

The information stored in clastic cave sediments has been poorly explored relative to the more commonly studied chemical precipitates. Clastic cave sediments have the potential to provide evidence relevant to paleoclimate (Panno et al. 2004, White 2007, van Hengstum et al. 2010), elemental cycling (Vesper and White 2003, Hartland et al. 2012), subterranean ecosystems (Birdwell and Engel 2010, Pipan and Culver 2013, Husic et al. 2017, de Paula et al. 2020), paleohydrology (Granger et al. 2001, McCloskey and Keller 2009, Chess et al. 2010, Polk et al. 2013), and contaminant storage (Vesper and White 2004, Mahler et al. 2007, Torres et al. 2018). Organic carbon is a controlling factor in many of these processes, however, organic carbon concentrations in clastic cave deposits are generally not reported. While spatiotemporal heterogeneity in flow regime, geomorphology, and water chemistry adds complexity, deposited cave sediments experience consistent environmental conditions compared to subaerial fluvial systems (Bull 1981, de Paula et al. 2020). This property makes cave sediments valuable environments to explore organic matter dynamics between systems with differing hydrogeology.

Clastic cave sediments include all materials not precipitated in-situ. These may include detrital matter derived from the weathering of the host rock or surface-derived material (White 1988, Bosch and White 2007). The latter is generally considered to be the dominant source of clastic sediments and its introduction may be associated with collapsed structures such as sinkholes, in response to major storms, or associated with more global climate changes. Surface-derived sediments are transported into a system via gravity or associated with incoming recharge flow (Hart and Schurger 2005). These surface-derived sediments are injected and subsequently deposited in the subsurface where they are relatively protected from the erosive processes occurring at the surface. During speleogenesis, a cave system may undergo cycles of sediment accumulation and erosion in response to external forcing due to climatic events or, on a longer time scale, glacial and inter-

glacial cycles (Anthony and Granger 2007, Farrant and Smart 2011, Asanidze et al. 2017). Geomorphological and land use changes may also alter the types and volumes of input from the surface.

Sedimentary deposits within fluvial systems are a known carbon sink, storing organic carbon introduced from upland areas (Martínez-Mena et al. 2019). Terrestrial organic carbon transport within a fluvial system is positively related to the onset of suspended sediment and in turn the erosive processes occurring within the catchment area (Galy et al. 2015). Cave systems are the subterranean equivalent of river systems where materials from upland areas are transported and deposited within a natural sink (Ford and Williams 2007, Nichols 2009). While the sediment carrying capacity of cave systems is significantly less (with some exceptions) than that of fluvial systems, sediment transport is sustained for longer periods of time after a hydrologic event (Husic et al. 2017). Recent works have shown that organic carbon concentrations associated with suspended sediment are a potentially significant pool of carbon in cave systems (McCarthy and McKay 2004, Cruz et al. 2005, Simon et al. 2007, Ban et al. 2008, Hartland et al. 2012, Husic et al. 2017). Deposited sediments are found in nearly all cave systems, and while suspended sediment as a carbon source has been explored, organic carbon associated with deposited cave sediments remains largely unreported.

Sediment input into a cave is episodic and the sediments may continue to persist with limited alteration due to relatively consistent environmental conditions and lack of sunlight. Work by Rossel et al. (2013) revealed that microbial activity in the absence of light played a significant role in organic carbon transformation. While the lack of light eliminates phototropic microbial activity, it has been demonstrated that alternative metabolic processes can flourish in these ambient, oligotrophic conditions (Simon et al. 2003, Engel 2007, Birdwell and Engel 2010, Ortiz et al. 2014, Galassi et al. 2016, Simon 2019, de Paula et al. 2020). The importance of microbial degradation and transformation of organic matter on the surface is well known, however, the role subterranean ecosystems play in carbon cycling within these systems remains poorly quantified (Butman et al. 2007, de Paula et al. 2020). Recent work has shown that initial chemical composition has little control on natural organic matter transformation but rather depends on the depositional environmental conditions (Schmidt et al. 2011, Marín-Spiotta et al. 2014, Martínez-Mena et al. 2019). Sediment organic carbon stored under ambient conditions within a cave could provide important insights into how and why environmental conditions play such an important role in organic matter transformation.

The sediments in this study were collected from the northern karst region of Puerto Rico, where abundant groundwater resources have promoted industrial and urban development, resulting in 25 Superfund sites on the EPA National Priority List (Padilla et al. 2001). Groundwater contamination in this region of Puerto Rico includes chlorinated volatile organic compounds (CVOCs), pesticides, and heavy metals. Although concentrations have decreased over time, contamination has persisted for more than 40 years (Yu et al. 2015, Torres et al. 2019). The concentration of organic matter present in a sediment is one of the primary controls on how organic contaminants are partitioned between the sorbed and dissolved phase (Schwarzenbach et al. 2016). Storage of sediment organic carbon within a karst system has important implications for contaminant transport and storage. Extreme weather events, such as hurricanes, could mobilize previously deposited subsurface sediments and stored contamination, resulting in potential human exposure to harmful compounds. The organic carbon data from cave systems in Puerto Rico reported in this study will help predict the long-term contaminant fate and support potential future remediation efforts.

In this study, organic carbon concentrations were obtained for clastic sediments from two caves in Puerto Rico with different surface connections and hydrological properties. The goal of this study was to determine the range and distribution of organic carbon in cave sediments along with potential correlations between carbon and sedimentological or hydrological properties. Paired nitrogen data were obtained in order to further characterize the sediment organic carbon using total organic carbon (TOC) and total organic nitrogen (TON) ratios. This study demonstrates the presence of carbon in cave sediments has a wider range than concentrations reported from suspended cave sediment and dissolved organic carbon (DOC) within cave streams. Despite the differing hydrologic conditions between the two cave systems, sediment TOC concentrations were comparable. The presence of organic carbon within deposited cave sediments is an important carbon reservoir that future works should consider regarding subsurface carbon cycling and contaminant transport.

## Location Information And Methods

# Sample locations and collection

Sediments were collected from two caves located in the northern karst region of Puerto Rico: Tallonal (TAL) Cave and Cueva (CAM) Cave (Fig. 1a) in February 2019. This karst region is eogenetic, having undergone little to no post-depositional deformation (Giusti 1978). A total of 13 cores from TAL and 9 cores from CAM were collected. The sediment cores were subsampled for analysis, resulting in 89 and 59 individual sediment samples from TAL and CAM caves, respectively.

TAL Cave is comprised of one main sinusoid passage, approximately 60 m in length, with no branching side passages, no known upper or lower levels, and a continuously flowing cave stream (Fig. 1b). Water enters the cave from an upward-flowing sump spring in the back of the cave and flows downstream to the cave entrance (Fig. 2a). A datalogger installed at TAL shows that turbidity coincides with most rain events (F. Pantoja-Agred, pers. comm., January 5, 2016). A dam at the cave entrance supports a private water supply and fixes the base water level in the cave. The dam is periodically opened to flush the system, manage storm surges, or to allow access to the cave.

Samples were collected from sediment banks located approximately 25 meters from the entrance of TAL Cave (Fig. 2a). The sediment bank in this room contains an erosional terrace which has been interpreted as the baseflow water level when the dam is closed (Fig. 2a). To compare between samples, the ceiling height in the room was defined as an arbitrary datum and all sediments were given a vertical location relative to that datum (Fig. 2b). Based on the height of the terrace, the dammed water level in the cave is 137 cm below datum. Samples collected below the terrace are considered saturated (typically underwater); those collected above the terrace level are considered unsaturated (typically above water, Fig. 2b). Small (< 2 cm thick) speleothem deposits were observed on top of the sediment bank suggesting that the sediment deposit is not new. Because the angle of the core samples relative to the bank could not be consistently maintained, the sediment cores are not stratigraphically consistent and an accurate correlation between the cores could not be determined; thus is not included in the assessment (Fig. 2c).

The second sampling location, CAM, is operated by a National Parks Company and is part of a natural protected area designated by the Commonwealth of Puerto Rico (Fig. 1c). CAM is a toured portion of the Camuy cave system. The Río Camuy cave system contains multiple dry-cave levels that were left behind as the Río Camuy River baseflow lowered and diverted deeper underground (Miller 2009). The Río Camuy River is currently at the base of a large sinkhole approximately 20 meters below the CAM sample locations (Fig. 1d). CAM samples location is a dry cave due to the vertical abandonment of the Río Camuy River, a subterranean river within the northern karst region of Puerto Rico (Fig. 1d). Cave sediments from the uppermost levels of the Río Camuy Cave system, dated using cosmogenic isotopes ($^{10}$Be and $^{26}$Al), have been in place for up to 4.5 million years (Miller et al. 2017).

On September 20, 2017, Hurricane Maria made landfall on Puerto Rico. The storm surge combined with a tidal swell produced a maximum surge of 1.5 meters along the northern coast. Over 2.3 meters of rainfall fell on the island in just over 32 hours (Pasch et al. 2017). The Río Camuy River level rose at least 20 meters as a result of Hurricane Maria completely flooding the generally dry room (Miller 2018). Once the river returned to baseflow after the storm, approximately 0.4 meters of sediment was deposited throughout the cave. The new sediment was clearly identified because it accumulated on the paved walkways used for the public tour. All sediments included in this study were collected after Hurricane Maria.

# Sample preparation and laboratory methods

Core samples were collected by pushing a 5 x 30.5 cm polyethylene core sleeve into the sediment. After collection, the cores were capped, wrapped, refrigerated, and kept from direct light until analysis.

In the laboratory, the core sleeves were split in half with a straight edge blade exposing two clean core faces for subsample collection. Subsamples were collected for analysis from 1 ± 0.5 cm sections of the core at depths in which visible change had occurred (e.g. color, grain size, or density changes). Subsamples for particle size analysis were prepared using a 1:1.5 sediment to 5% Calgon® solution mass ratio to minimize clumping, then placed on a rotary shaker overnight at 70 rpm. Sediment slurries were analyzed using a Beckman Coulter single wavelength LS13-320 particle size analyzer that measures sizes between 0.4 µm and 2,000 µm. Particle size is reported as a volume percent. Raw data files from the instrument were organized via R and processed through the GRADISTAT program (Blott and Pye 2001).

Subsamples collected for carbon and nitrogen were homogenized, air dried for 24 hours, and subsequently oven dried at 60°C for another 24 hours. Total carbon (TC) and total nitrogen (TN) were determined using a Carlo Erba NA1500 CNHS elemental analyzer at the University of Florida's Stable Isotope Mass Spectroscopy Laboratory. Total inorganic carbon (TIC) was determined by acidifying the sediment under an $N_2$ blanket. Evolved $CO_2$ resulting from the acidification was then quantified coulometrically using a UIC 5017 $CO_2$ coulometer. Total organic carbon (TOC) was determined as the difference between TC and TIC.

## Results

# Physical properties

Apparent layering observed in TAL was a result of variation in cohesiveness rather than grain size (Fig. 3). Following the Folk and Ward (1957) devised sorting scale (unitless), sediments collected from TAL were categorized as poorly to extremely poorly sorted (poorly sorted: 1.0–2.0; very poorly sorted: 2.0–4.0; extremely poorly sorted: >4.0). TAL sediments were, on average, categorized as extremely poorly sorted (average 4.3) whereas CAM sediments were very poorly sorted (average 3.2). Due to the poorly sorted nature of the sediments, proportions of sand, silt, and clay are referenced rather than mean grain size. Sediments from both cave locations contained dominantly fine sand to coarse silt sized grains. Proportion of sand from TAL sediments (average 50.2%) was significantly higher than CAM sediments (average 38.9%; $p$ value < 0.05). No significant differences ($p$ value < 0.05) in grain size were observed between saturated and unsaturated sediments from TAL location 16 (Fig. 4).

Discontinuous thin banding of a black material was present throughout core TAL 16 − 04 (Fig. 3b). This core was in contact with the water table and experienced saturation in response to fluctuations in stream water level (Fig. 2). Preliminary XRF data were collected on a select number of grab samples for semi quantitative characterization using the mudrock calibration created by Rowe et al. (2012). This preliminary analysis showed elevated levels of Mn and Fe (molar units, > 2σ of the mean), common redox sensitive oxide forming elements, in sediments from core 16 − 04 (Downey 2020). Precipitation of Fe or Mn oxides could be a possible explanation for the black banding present in core 16 − 04 (Fig. 3c).

The remaining cores collected from location 16 were fully saturated (Fig. 2b). Variable color zonation was present in all saturated cores (Fig. 3c). These zones ranged in size and the contacts between zones were variable in shape and clarity. Color within these zones ranged from a dark brown or dark green hue to lighter tan (Fig. 3c). All samples collected from location 17 were saturated and showed similar color variation to the saturated cores collected from location 16 (see supplementary Fig. S1). Small (< 2 cm thick) stalagmite deposits coating portions of the sediment bank near sample location 16 was observed, indicating that these sediments have been in place for some time.

Sediment cores were collected throughout CAM (Fig. 1c). In general, CAM sediments contained more distinct sedimentary layering than those collected from TAL (see supplementary Fig. S2). The CAM cores varied significantly between sample locations with no observable stratigraphic correlation. Large desiccation cracks covered the sediment surface throughout CAM, suggesting that the sediments were not saturated after their initial deposition via Hurricane Maria.

# Chemical properties

The concentrations of TOC (wt%) ranged from 0.13 to 0.73 (average 0.33, n = 22) in unsaturated TAL samples and from 0.11 to 2.36 (average 0.96%, n = 71) in saturated TAL samples (Fig. 5a). TOC concentrations ranged from below detection to 3.43% (average 0.42%, n = 59) in CAM sediment samples. Combined TAL saturated and unsaturated sediment TOC (average = 0.8%) concentrations were, on average, twice as high as CAM sediments (Fig. 5a). TOC comprised most of the total carbon in samples from TAL (average 83%) with a strong linear relationship ($R^2$ = 0.97 $p$ value < 0.05) between TOC and TC (Fig. 5b). There was no relationship between TOC concentration and proportion of sub-silt sized grains at either location 16 or 17 in TAL sediments or CAM sediments ($R^2$ = 0.025 $p$ value < 0.05). TOC made up a lesser proportion of the total carbon in CAM (average 70%). Of the 59 samples analyzed from CAM, 19 contained less than 40% of the carbon in the organic form

(Fig. 5b). Whereas, of the 89 samples collected from TAL, only one sample contained less than 40% of carbon in the organic form (Fig. 5b).

Concentrations of TOC were significantly higher in saturated sediments from TAL ($p$ value < 0.01) relative to either unsaturated TAL or CAM samples (Fig. 5a). TOC concentrations from TAL sediments, when plotted against depth relative to the datum, reveal a sharp increase in TOC concentration at the inferred stream level (Fig. 6). The sharp increase in TOC concentration between unsaturated and saturated sediments present in TAL sediments could not be evaluated in the CAM sediments because those sediments were not saturated after their initial deposition. The TOC variation between unsaturated and saturated TAL sediments suggests that the presence or absence of water in the sediments plays a role in carbon storage and/or carbon generation after initial input into the system.

Complementary TN data collected for all sediments provides a framework for initial sediment organic carbon characterization. A strong linear relationship exists between TOC and TN in both saturated ($R^2$ = 0.82 $p$ value < 0.05) and unsaturated ($R^2$ = 0.65 $p$ value < 0.05) TAL sediments. Following the method of Goni et al. (1998), total inorganic nitrogen (TIN) can be estimated from TOC by applying a linear regression to a TN vs. TOC plot. The concentration of TIN ($C_{TIN}$) is mathematically represented by the y-intercept. $C_{TIN}$ was estimated to be 0.036 ($C_{TIN}$=0.08$C_{TOC}$ + 0.036) and 0.042 ($C_{TIN}$=0.10$C_{TOC}$ + 0.042) for saturated and unsaturated sediments from TAL, respectively. Like TAL sediments, TOC and TN were strongly correlated ($R^2$ = 0.77 $p$ value < 0.05) in sediments from CAM. However, the y-intercept was lower ($C_{TIN}$=0.10$C_{TOC}$ + 0.015). This reveals that CAM sediments contained less TIN than TAL sediments.

By subtracting the estimated TIN from TN, total organic nitrogen (TON) can also be estimated ($C_{TON}$=$C_{TN}$-$C_{TIN}$). From this, TOC:TON molar ratios were calculated. Average TOC:TON ratios were 17.7 (standard deviation, SD = 13.4) and 13.70 (SD = 10.1) for saturated and unsaturated TAL sediments, respectively (Fig. 7). Average TOC:TON from sediments collected at CAM was 15.9 (SD = 12.4). The high SD calculated from the TOC:TON ratios from each cave location hints at the heterogeneous nature of natural organic matter. Despite this, average TOC:TON values are still informative for initial organic matter characterization and comparison to standard types of natural organic matter. Humic and fulvic acids, a major component of natural organic matter, average C:N ratios are 18.0 and 20.4, respectively (Rice and MacCarthy 1991, Essington 2015). Amino acids, the main component of non-humic like natural organic matter, has a lower average C:N ratio at 3.15 (Jover et al. 2014). TOC:TON ratios collected from sediments at both locations show ratios within the range of humic and fulvic acids, independent of TOC concentration (Fig. 7). Highest TOC:TON values were found in cave sediments with lower TOC concentrations at both TAL and CAM locations. TOC:TON ratio values consistent with amino acids were observed only in CAM sediments.

## Discussion

# Variability between cave systems

Sediment mobility within a conduit is dependent on cave morphology, groundwater flow, the magnitude of rain events, and flow velocity; most karst systems are likely to contain both gradual and threshold-based changes (Herman et al. 2008). The hydrogeology of the two cave systems included in this study are very different. TAL

is a wet cave with a continuously flowing cave stream; in contrast, CAM does not have flowing or perennial water in the upper (older) level of the Río Camuy system from where samples were collected (Miller et al. 2017). The cave stream flowing through TAL becomes turbid during most rain events whereas sediment input at CAM occurs only when the Río Camuy River rises to reach the dry cave, as it did during Hurricane Maria. While the cave stream in TAL frequently carries suspended sediment, the relationship between turbidity, deposition, and remobilization remains under investigation. Stalagmites (< 2 cm thick) coating portions of the sampled sediment banks was observed, indicating the deposited sediments have been in place at TAL for an extended time. The sediments collected from CAM were known to be deposited by flooding via the Río Camuy River resulting from Hurricane Maria. These sediments have not been reworked since deposition and were in place approximately 18 months at the time of sampling. TOC variation between the two caves reflects the differences in sediment sources, input dynamics, and post depositional conditions. The data reported in this study suggest that sediment saturation plays an important role in carbon storage within the subsurface.

The heterogeneity of a sedimentary environment facilitates the presence of microenvironments leading to variations in limiting nutrients and electron acceptors. Work by Schlüter et al. (2018) showed that conditions change from anoxic to oxic surrounding a sediment particle in just over 0.4 mm. Redox zonation results from variation in oxygen availability and the thermodynamic availability of electron acceptors in an environment. The semi quantitative elemental XRF analysis suggests that the black banding present in TAL 16 – 04 is possibly microcrystalline Mn oxide banding (Downey 2020). This is likely from fluctuation in water level as Mn oxides rapidly precipitate when environments transition from suboxic to oxic (Dixon et al. 1990) (Fig. 3b). The electromotive potential of a soil has been correlated to the characteristics of the pore water solution within a sedimentary environment (Wanzek et al. 2018). Chess et al. (2010) described sediment facies from Butler Cave, VA as “low and wet” and “high and dry” based on color variation attributed to varying degrees of hydration of iron oxides. Sediment saturation in TAL Cave could enhance the redox conditions within the sediments resulting in precipitation reactions causing the colored zonation observed in nearly all saturated sediment cores (Fig. 3c).

Organic carbon was significantly higher in saturated sediments compared to unsaturated sediments in TAL. Work by Cruz et al. (2005) found that organic carbon concentrations were highest in more reducing conditions, linking organic carbon to redox conditions in the subsurface. In addition to facilitating enhanced electromotive potential, pore water is the principal mode of transport for materials into and out of these sediments. The exchange and transport of surface derived organic matter, including DOC, is likely occurring between the water column and the sediment pore solution. The transport of surface derived organic carbon into deposited sediment pore water could facilitate long term storage and subsequent transformation and/or mineralization.

TOC:TON ratios differed between cave systems. TOC:TON ratios consistent with amino acids were found only found in CAM sediments. Amino acids typically represent protein like organic matter when evaluating spectrographic data and has historically been interpreted as a microbial signature (Coble 1996). Saturated TAL sediments contained slightly higher TOC:TON values (average, 17.7), closer to a humic acid-like signature. This is, however, not evidence that TAL lacks a microbial signature. The exact structure and composition of natural organic matter is complex and not well defined. Therefore, categorizing the organic matter within these sediments has humic acid-like, fulvic acid-like, or amino acid-like based on TOC:TON ratio values are shown in Fig. 7 as an exploratory comparison to accepted values for various known types of organic carbon. These data

are provided as a framework for comparison. Moreover, the calculated TOC:TON ratios from both caves had relatively large standard deviations (Fig. 7). The high variability in TOC:TON ratios in sediments collected from the same cave, some only centimeters apart is likely due to the complex and heterogeneous nature of natural organic carbon.

# Comparison of organic carbon concentrations to similar sites

Despite the complexity of sedimentary organic matter, TOC:TON is a widely reported parameter and the analyzed cave sediments in this study enables a useful preliminary comparison to other soil and sediment datasets (Table 1). In general, higher TOC:TON ratios indicate liable organic matter (vascular plants and woody materials). Lower values are typically indicative of carbon mineralization. Average TOC:TON ratios (TAL: 17.5, CAM: 15.9) from the cave sediments collected in this study are consistent with the liable fraction of organic matter. Work by von Fischer and Thiessen (1995) reported TOC:TON ratio values collected from soil within the Luquillo Experimental Forest in eastern Puerto Rico within range of TOC:TON values collected in this study (Table 1). TOC:TON ratios from cave sediments reported by Fichez (1990) were lower than TAL and CAM sediments. This is, to our knowledge, the only study on cave sediments that report TOC:TON values for comparison.

Table 1

Organic carbon concentrations reported from sediments collected from a variety of geographic locations. Each set of data is referenced to the corresponding number plotted in Fig. 8. Note that some organic carbon concentrations are for dissolved organic carbon rather than sediment organic carbon.

| Figure 8 plot # | | Sample medium | Type of data | OC[a] min | OC[a] max | C/N | Location | Reference |
|---|---|---|---|---|---|---|---|---|
| This study | 1 | deposited cave sediment | SOC[b] (wt%) | 0.11 | 2.36 | 17.5[f] | TAL (this study) | |
| | 2 | deposited cave sediment | SOC[b] (wt%) | < DL[e] | 3.43 | 15.9[f] | CAM (this study) | |
| Cave sediment | 3 | deposited cave sediment | SOC[b] (wt%) | 0.02 | 0.50 | — | Illinois, USA | Panno et al. (2004) |
| | 4 | deposited cave sediment | SOC[b] (wt%) | 0.01 | 0.05 | — | Terra Ronca, Brazil | de Paula et al. (2020) |
| | 5 | deposited cave sediment | SOC[b] (wt%) | 3.30 | 3.50 | 10.0 | Marsielle, France | Fichez (1990) |
| | 6 | suspended cave sediment | SOC[b] (wt%) | 2.00 | 8.20 | — | Kentucky, USA | Husic et al. (2017) |
| | 7 | suspended cave sediment | SOC[b] (wt%) | 0.38 | 3.37 | — | Derbyshire, UK | Bottrell (1996) |
| Cave water | 8 | Cave stream | DOC[c] (mg/L) | 1.20 | 3.40 | — | West Virginia, USA | Simon et al. (2003) |
| | 9 | Cave stream | DOC[c] (mg/L) | 1.08 | 4.75 | — | West Virginia, USA; Slovenia | Simon et al. (2007) |
| | 10 | Cave stream | DOC[c] (mg/L) | 0.20 | 9.30 | — | West Virginia, USA | Simon et al. (2010) |
| | 11 | Cave stream | DOC[c] (mg/L) | 5.00 | 10.5 | — | São Paulo City, Brazil | Cruz et al. (2005) |
| | 12 | Cave dripwater | DOC[c]; POC[d] (mg/L) | 1.70 | 3.00 | — | Gloucestershire, UK; Derbyshire, UK; Trentino, Italy | Hartland et al. (2012) |
| Surface water and sediment | 13 | soil pore water | DOC[c] (mg/L) | $2.44 \times 10^{-4}$ | $5.26 \times 10^{-4}$ | — | Luquillo Forest, PR | McDowell (1998) |
| | 14 | river | POC[d] (wt%) | $1.00 \times 10^{-5}$ | $3.33 \times 10^{-3}$ | — | Rio Loco, PR | Moyer et al. (2013) |

| Figure 8 plot # | Sample medium | Type of data | OC[a] min | OC[a] max | C/N | Location | Reference |
|---|---|---|---|---|---|---|---|
| 15 | soil | SOC[b] (wt%) | 1.40 | 4.60 | 17.9 | Luquillo Forest, PR | von Fischer and Tieszen (1995) |
| 16 | suspended river sediment | SOC[b] (wt%) | 4.48 | 14.2 | — | San Juan Bay, PR | Pérez-Villalona et al. (2015) |
| 17 | wetland sediment | SOC[b] (wt%) | 1.10 | 35.6 | 22.0 | San Juan Bay, PR | Eagle et al. (2021) |
| 18 | suspended river sediment | SOC[b] (wt%) | 0.08 | 4.09 | 13.5 | Luzon Island, Philippines | Lin et al. (2021) |

[a] organic carbon

[b] sediment organic carbon

[c] dissolved organic carbon

[d] particulate organic carbon

[e] below detection limit

[f] average value

Sediment organic carbon collected from TAL and CAM in this study were compared with other cave sediments from various locations (Table 1; Fig. 8). Of the five studies that report cave sediment organic carbon compiled for comparison, three were collected from deposited cave sediments and the remaining two report sediment organic carbon associated with suspended sediment from a cave stream (Table 1). Studies reporting on suspended cave sediments reveal higher overall TOC concentrations than those reporting on deposited cave sediments. Husic et al. (2017) demonstrated that organic carbon associated with suspended sediments decreased from input to output through a cave stream suggesting some form of retention within the system (Fig. 8; Table 1). Paula et al. (2020) reported deposited cave sediment organic carbon and found that higher concentrations occurred during the tropical wet seasons from a cave in Brazil. CAM sediments had the largest range and lowest concentration of TOC. This is also the only cave in the compiled dataset known to be dominantly dry year-round. This, coupled with higher TOC values associated with suspended cave sediments (Table 1; Fig. 8) corroborates the idea that sediment saturation is an important control on organic carbon deposition and subsequent storage within cave systems.

DOC concentrations within cave streams from a variety of locations have also been reported and are included for comparison (Table 1; Fig. 8). DOC concentrations within these cave streams are comparable the compiled suspended sediment organic carbon data. Values of DOC reported from cave water are only slightly higher than TOC sediment concentrations collected in this study and reported in the literature(Table 1: lines 1–4). The cave

sediment data compiled here lead to the conclusion that TOC associated with sediments are a significant additional pool of organic carbon within the subsurface and should be considered when quantifying carbon fate and transport in the subsurface.

Surface soils are an important sink for carbon storage (Essington 2015). Tropical climates promote abundant vegetation and rapid soil carbon turnover (Sayer et al. 2019). Work by Moyer et al. (2013) analyzed small mountain streams throughout Puerto Rico and found that organic matter is rapidly mobilized and subsequently stored within the coastal floodplains due to the abundant rainfall occurring on the island. Due to the efficient surface to groundwater transfer occurring within the Puerto Rico karst region, it is assumed that some of this sediment and associated organic carbon will make it into the groundwater system. The TOC values reported in this study were compared to various tropical sediments and soils, including from Puerto Rico (Fig. 8; Table 1). River POC and soil pore water DOC collected from central Puerto Rico were significantly lower than any of the reported cave sediment concentrations (number 14 and 15 in Fig. 8). While only a few studies from surface sediments and soils are reported here for comparison, cave sediment TOC concentrations are within range of these values, further illustrating the importance of organic carbon in the subsurface.

# Implications for contaminant fate and transport

The organic carbon associated with deposited sediments has important implications for contaminant fate and transport in a karst aquifer. The organic carbon-water partition coefficient ($K_{iocw}$) is used to quantify the affinity of a given chemical, *i*, for natural organic matter (Schwarzenbach et al. 2016). Due to the complex, apolar structure of most natural organic matter, it often exhibits a high sorption affinity for most aromatic organic contaminants. Consequently, the solid-water partition coefficient ($K_{id}$) of a chemical, *i*, is proportional to the concentration of organic carbon within the sedimentary environment (Table 2). The presence of fine-grained sediments and natural organic matter in a groundwater flow path with known organic contamination increases the possibility of retention or storage through sorption. The retention of an organic contaminant is often quantified by calculating the ratio of the average linear velocity of groundwater to the velocity of the contaminant, referred to as a retardation factor. Higher retardation factors suggest that the transport of a chemical will be slower than groundwater flow.

Table 2
Common contaminants found in Puerto Rico groundwater with estimated organic carbon-water coefficient (Kiocw) and retardation factors

| Contaminant name[a] | Abbreviation | log $K_{iocw}$[b] | log $K_d$ (min)[c,d] | log $K_d$ (max)[c,d] | $R_{fi}$ (min)[d,e,f] | $R_{fi}$ (max)[d,e,f] | % Increase[g] in $R_{fi}$ |
|---|---|---|---|---|---|---|---|
| Trichloroethylene | TCE | 2.22 | -1.47 | 0.59 | 1.05 | 7.18 | 582 |
| Tetrachloroethylene | PCE | 2.19 | -1.51 | 0.56 | 1.05 | 6.77 | 545 |
| Chloroform | TCM (or CF) | 1.60 | -2.09 | -0.03 | 1.01 | 2.48 | 145 |
| Carbon tetrachloride | CCl4 (or CT) | 2.24 | -1.46 | 0.61 | 1.05 | 7.47 | 608 |
| 1,1-Dichloroethane | 1,1-DCA | 1.5 | -2.20 | -0.13 | 1.01 | 2.18 | 116 |
| *Cis*-1,2-Dichloroethylene | CIS-1,2-DCE | 1.55 | -2.15 | -0.08 | 1.01 | 2.32 | 129 |
| 1,2-Dichloroethane | 1,2-DCA | 1.24 | -2.46 | -0.39 | 1.01 | 1.65 | 63.8 |
| 1,1,1-Trichloroethane | 1,1,1-TCA | 2.04 | -1.66 | 0.41 | 1.03 | 5.08 | 391 |
| 1,1,2-Trichloroethane | 1,1,2-TCA | 1.70 | -2.00 | 0.07 | 1.02 | 2.86 | 182 |
| 1,1,2,2-Tetrachloroethane | 1,1,2,2-TeCA | 1.97 | -1.73 | 0.34 | 1.03 | 4.48 | 335 |
| *Trans*-1,2-Dichloroethylene | Trans-1,2-DCE | 1.72 | -1.98 | 0.09 | 1.02 | 2.96 | 191 |
| Vinyl chloride | VC | 1.27 | -2.43 | -0.36 | 1.01 | 1.69 | 68.4 |
| Bromoform | BF | 1.94 | -1.76 | 0.31 | 1.03 | 4.24 | 313 |
| Bromodichloromethane | BDCM | 1.74 | -1.96 | 0.11 | 1.02 | 3.05 | 199 |
| Chlorodibromomethane | CDBM | 1.80 | -1.90 | 0.17 | 1.02 | 3.35 | 228 |

[a]common contaminants found in Puerto Rico groundwater; data compiled from Torres et al. (2019)

[b]organic carbon-water partition coefficient: $K_{id} = \frac{C_{is}}{C_{iw}}$ where $C_{is}$ is the concentration of compound *i* sorbed to a solid and $C_{iw}$ is the concentration of compound *i* in the dissolved phase; data compiled from EPA (1996)

[c]$\log(K_{id}) = \log(f_{oc} K_{iocw})$ where $f_{oc} = \frac{mass\ of\ organic\ carbon}{total\ mass\ of\ solid}$

[d]min $f_{oc}$ value of 0.0002; max $f_{oc}$ value of 0.0236 based on min and max organic carbon concentrations collected in this study

[e]bulk density of silty sediments $\rho_s = 1.78$; porosity of silty sediments $\varphi = 0.53$; values from Manger (1963)

| Contaminant name[a] | Abbreviation | log $K_{iocw}$[b] | log $K_d$ (min)[c,d] | log $K_d$ (max)[c,d] | $R_{fi}$ (min)[d,e,f] | $R_{fi}$ (max)[d,e,f] | % Increase[g] in $R_{fi}$ |
|---|---|---|---|---|---|---|---|
| [f]retardation factor: $R_{if} = 1 + (\rho_s / \varphi) K_{id}$ where $\rho_s = 1.78$ (density of the solid) and $\varphi = 0.53$ (porosity of the solid) | | | | | | | |
| [g]percent increase in retardation factor between the minimum and maximum organic carbon concentrations | | | | | | | |

The high solid-water partition coefficients, controlled by the concentration of natural organic matter, lead to higher retardation factors (Table 2). Concentrations of TCE, $CCl_4$, and PCE are among the highest detected contaminants in Puerto Rico's groundwater (Torres et al. 2019). The fraction of organic carbon ($f_{oc}$) within the cave sediments collected in this study ranged from 0.0002–0.0236. The presence of $f_{oc}$=0.0236 (maximum found in this study) would increase the retardation of TCE, $CCl_4$, and PCE by 582, 608, and 545%, respectively, when compared to the minimum $f_{oc}$ found in this study (Table 2). Natural organic matter associated with sediments within an aquifer may account for significant sorption and storage of organic compounds in groundwater; this sorption has been cited as a possible reason for the persistence of contamination within a karst aquifer (Padilla and Vesper 2018, Torres et al. 2019).

Work by Lin et al. (2020) found that concentrations of CVOC contaminants in Puerto Rico's drinking water increased significantly following Hurricane Maria. While sorption removes contaminants from the water column, large storm events such as Hurricane Maria will result in severe flooding potentially mobilizing previously deposited sediments and any associated sorbed contaminants. These mobilized sediments act as a vector for contaminant transport, potentially entering public or private water supplies (Mahler et al. 2007).

# Conclusions

Organic carbon associated with suspended sediment within a cave system as a potentially significant pool of organic carbon has been studied, however, deposited cave sediments as an organic carbon pool has remained largely unexplored. The results from this study show that concentrations of organic carbon within deposited cave sediments are within the range of organic carbon associated with suspended cave sediments or DOC within the groundwater. Sediments and associated organic carbon from CAM were deposited recently via Hurricane Maria and have not been reworked since, whereas the TAL cave stream experiences turbidity during most rain events. Organic carbon concentrations varied significantly (p value < 0.05) between cave systems. The range in organic carbon concentrations within TAL sediment was lower than CAM sediments but contained on average higher concentrations of organic carbon. These differences are likely controlled by many factors, including but not limited to, post-depositional metabolic activity, redox, ambient environmental conditions, and time. The TOC:TON ratios of the collected cave sediments are consistent with terrestrial materials and comparable to TOC:TON ratios of sediments found in the central highlands of Puerto Rico.

Significant differences between unsaturated and saturated sediments from TAL were observed. It is highly likely that the colored zonation present saturated TAL sediments are a result of changing redox conditions facilitating precipitation of some redox sensitive minerals. In addition to the colored zonation, organic carbon

was significantly higher in TAL saturated sediments. Sediment pore solution is the most dominant mode of transport for freshly input organic matter to enter a subsurface sedimentary environment. However, exact mechanism resulting in the higher concentrations of organic carbon in the saturated sediments from TAL remains under investigation.

It is important to remember that organic carbon concentrations from only two caves are reported here. Given the heterogeneity in karst systems, this is unlikely to provide a full range of conditions and carbon concentrations. However, this study does add to our knowledge about the distribution and range of TOC concentrations in these systems which provides important information to direct future work. The bulk organic carbon concentrations from the cave sediments reported in this study show that organic carbon associated with long term subsurface sedimentary environments is significant enough to warrant the inclusion of such deposits when attempting organic carbon flux calculations.

The presence of natural organic carbon in the subsurface is exceptionally important for contaminant transport. Retardation factors calculated using the minimum and maximum organic carbon concentrations collected from the sediments in this study reveals drastic increases in retardation of common contaminants found in Puerto Rico's groundwater. The sorption of organic contaminants onto the karst aquifer organic matter also contributes to the long-term storage of contamination in this system. This may play an important role for remedial design and for public health concerns in the region.

## Declarations

# Funding

This project was supported by the Puerto Rico Testsite for Exploring Contamination Threats (PROTECT) Program (award number P42ES017198), a project funded by the National Institute of Environmental Health Sciences' Superfund Research Program.

# Data

The data obtained from this project is included as a supplemental table to this manuscript.

# Competing interests

The authors have no completing interests.

# Authorship contributions

**Autum R Downey**: Investigation, Conceptualization, Methodology, Writing, Revision. **Jill L Riddell:** Investigation, Writing – Review and Editing. **Ingrid Y Padilla**: Writing – Review and Editing. **Dorothy J Vesper**: Conceptualization, Methodology, Revision, Editing, Supervision.

# Acknowledgments

This project was supported by the Puerto Rico Testsite for Exploring Contamination Threats (PROTECT) Program (award number P42ES017198), a project funded by the National Institute of Environmental Health Sciences' Superfund Research Program. We appreciate Abel Vale and the organizations Ciudadanos Del Karso (the Citizens of Karst) and the National Parks Company of the Commonwealth of Puerto Rico for cave access. We would also like to thank University of Puerto Rico Fernando Pantoja-Agred for the Tallonal data and Ángel A. Acosta-Colón for field support and logistical planning. We also thank Dr. Ellen Herman, Dr. Brian Smith, Omar Rodriguez, Tatiana Rosado, and Laura Rodriguez for field assistance and Anastasia Simpson and Mathew Bell for lab assistance.

# References

1. Anthony DM, Granger DE (2007) A new chronology for the age of Appalachian erosional surfaces determined by cosmogenic nuclides in cave sediments. Earth Surf Processes Landf 32:874–887. https://doi.org/10.1002/esp.1446
2. Asanidze L, Chikhradze N, Lezhava Z, Tsikarishvili K, Polk J, Chartolani G (2017) Sedimentological study of caves in the Zemo Imereti Plateau, Georgia, Caucasus Region. Open J Geol 07:465–477. https://doi.org/10.4236/ojg.2017.74032
3. Ban F, Pan G, Zhu J, Cai B, Tan M (2008) Temporal and spatial variations in the discharge and dissolved organic carbon of drip waters in Beijing Shihua Cave, China. Hydrol Processes 22:3749–3758. https://doi.org/10.1002/hyp.6979
4. Birdwell JE, Engel AS (2010) Characterization of dissolved organic matter in cave and spring waters using UV–Vis absorbance and fluorescence spectroscopy. Org Geochem 41:270–280. https://doi.org/10.1016/j.orggeochem.2009.11.002
5. Blott SJ, Pye K (2001) GRADISTAT: a grain size distribution and statistics package for the analysis of unconsolidated sediments. Earth Surf Processes Landf 26:1237–1248. https://doi.org/10.1002/esp.261
6. de Paula CCP, Bichuette ME, Seleghim MHR (2020) Nutrient availability in tropical caves influences the dynamics of microbial biomass. Microbiologyopen 9:1044. https://doi.org/10.1002/mbo3.1044
7. Bosch R, White WB (2007) Lithofacies and transport of clastic sediments in karstic aquifers. In Studies of Cave Sediments: Physical and chemical records of paleoclimate (eds. Sasowsky ID, Mylroie J). pp 1–22. https://DOI:10.1007/978-1-4419-9118-8_1
8. Bull PA (1981) Some fine-grained sedimentation phenomena in caves. Earth Surf Processes Landf 6:11–22. https://doi.org/10.1002/esp.3290060103
9. Butman DE, Raymond PA, Oh N, Mull K (2007) Quantity, $^{14}C$ age and lability of desorbed soil organic carbon in fresh water and seawater. Org Geochem 38:1547–1557. https://doi.org/10.1016/j.orggeochem.2007.05.011
10. Chess DL, Chess CA, Sasowsky ID, Schmidt VA, White WB (2010) Clastic Sediments in the Butler Cave – Sinking Creek System, Virginia, USA. Acta Carsologica 39:11–26. https://doi.org/10.3986/ac.v39i1.109
11. Coble PG (1996) Characterization of marine and terrestrial DOM in seawater using excitation-emission matrix spectroscopy. Mar Chem 51:325–346. https://doi.org/10.1016/0304-4203(95)00062-3

12. Cruz FW, Karmann I, Magdaleno GB, Coichev N, Viana O (2005) Influence of hydrological and climatic parameters on spatial-temporal variability of fluorescence intensity and DOC of karst percolation waters in the Santana Cave System. Southeast Brazil Hydrogeol J 302:1–12. https://doi.org/10.1016/j.jhydrol.2004.06.012
13. Dixon JB, Golden DC, Uzochukwu GA, Chen CC (1990) Soil manganese oxides. In: de Boodt MF, Hayes MHB, Herbillon A, de Strooper EBA, Tuck JJ (eds) Soil Colloids and Their Associations in Aggregates. Springer US, Boston, MA, pp 141–163. https://doi.org/10.1007/978-1-4899-2611-1_7
14. Downey AR (2020) Physical and chemical properties of clastic sediments from two caves in the northern karst region of Puerto Rico. MS Thesis, West Virginia University, Morgantown West Virginia, USA. https://doi.org/10.33915/etd.7716
15. EPA (1996) Environmental Protection Agency. Soil Screening Guidance: Technical Background Document, 2nd ed. EPA/540/R95/128
16. Engel AS (2007) Observations on the biodiversity of sulfidic karst habitats. J Cave Karst Stud 69:187–206
17. Essington ME (2015) Soil and water chemistry: an integrative approach. 1st ed., Taylor and Francis Group. https://doi.org/10.1201/b12397
18. Farrant AR, Smart PL (2011) Role of sediment in speleogenesis; sedimentation and paragenesis. Geomorphology (Amst) 134:79–93. https://doi.org/10.1016/j.geomorph.2011.06.006
19. Folk RL, Ward WC (1957) A study in the significance of grain-size parameters. J Sed Petrol 27:3–26. https://doi.org/10.1306/74D70646-2B21-11D7-8648000102C1865D
20. Ford D, Williams P (2007) Karst Hydrogeology and Geomorphology. John Wiley and Sons, Ltd. https://doi.org/10.1002/9781118684986
21. Galassi DMP, Fiasca B, di Lorenzo T, Montanari A, Porfirio S, Fattorini S (2016) Groundwater biodiversity in a chemoautotrophic cave ecosystem: how geochemistry regulates microcrustacean community structure. Aquat Ecol 51:75–90. https://doi.org/10.1007/s10452-016-9599-7
22. Galy V, Peucker-Ehrenbrink B, Eglinton T (2015) Global carbon export from the terrestrial biosphere controlled by erosion. Nature 521:204–207. https://doi.org/10.1038/nature14400
23. Giusti E (1978) Hydrogeology of the karst in Puerto Rico. Geological Survey Professional Paper 1012
24. Goni MA, Ruttenberg KC, Eglinton TI (1998) A reassessment of the sources and importance of land-derived organic matter in surface sediments from the Gulf of Mexico. Geochim Cosmochim Acta 62:3055–3075. https://doi.org/10.1016/S0016-7037(98)00217-8
25. Hart EA, Schurger SG (2005) Sediment storage and yield in an urbanized karst watershed. Geomorphology (Amst) 70:85–96. https://doi.org/10.1016/j.geomorph.2005.04.002
26. Hartland A, Fairchild IJ, Lead JR, Borsato A, Baker A, Frisia S, Baalousha M (2012) From soil to cave: Transport of trace metals by natural organic matter in karst dripwaters. Chem Geol 304–305:68–82. https://doi.org/10.1016/j.chemgeo.2012.01.032
27. Herman EK, Toran L, White WB (2008) Threshold events in spring discharge: Evidence from sediment and continuous water level measurement. Hydrogeol J 351:98–106. https://doi.org/10.1016/j.jhydrol.2007.12.001

28. Husic A, Fox J, Agouridis C, Currens J, Ford W, Taylor C (2017) Sediment carbon fate in phreatic karst (Part 1): Conceptual model development. Hydrogeol J 549:179–193. https://doi.org/10.1016/j.jhydrol.2017.03.052
29. Jover LF, Effler TC, Buchan A, Wilhelm SW, Weitz JS (2014) The elemental composition of virus particles: implications for marine biogeochemical cycles. Nat Rev Microbiol 12:519–528. https://doi.org/10.1038/nrmicro3289
30. Lin Y, Sevillano-Rivera M, Jiang T, Li G, Cotto I, Vosloo S, Carpenter CMG, Larese-Casanova P, Giese RW, Helbling DE, Padilla IY, Rosario-Pabón Z, Vélez Vega C, Cordero JF, Alshawabkeh AN, Pinto A, Gu AZ (2020) Impact of Hurricane Maria on drinking water quality in Puerto Rico. Environ Sci and Technol 54:9495–9509. https://doi.org/10.1021/acs.est.0c01655
31. Mahler BJ, Personne JC, Lynch FL, van Metre PC (2007) Sediment and sediment-associated contaminant transport through karst. In Studies of cave sediments: Physical and chemical records of paleoclimate (eds. Sasowsky ID, Mylroie J). Springer. pp 23–46. https://doi.org/10.1007/978-1-4020-5766-3_2
32. Manger GE (1963) Porosity and Bulk Density of Sedimentary Rocks. United States Geological Survey Bulletin 1144-E
33. Marín-Spiotta E, Gruley KE, Crawford J, Atkinson EE, Miesel JR, Greene S, Cardona-Correa C, Spencer RGM (2014) Paradigm shifts in soil organic matter research affect interpretations of aquatic carbon cycling: transcending disciplinary and ecosystem boundaries. Biogeochem 117:279–297. https://doi.org/10.1007/s10533-013-9949-7
34. Martínez-Mena M, Almagro M, García-Franco N, de Vente J, García E, Boix Fayos C (2019) Fluvial sedimentary deposits as carbon sinks: Organic carbon pools and stabilization mechanisms across a Mediterranean catchment. Biogeosci 16:1035–1051. https://doi.org/10.5194/bg-16-1035-2019
35. McCarthy JF, McKay LD (2004) Colloid transport in the subsurface: past, present, and future challenges. Vadose Zone J 3:326–337. https://doi.org/10.2136/vzj2004.0326
36. McCloskey TA, Keller G (2009) 5000 year sedimentary record of hurricane strikes on the central coast of Belize. Quat Int 195:53–68. https://doi.org/10.1016/j.quaint.2008.03.003
37. Miller T (2009) Puerto Rico caves and karst. In Caves and Karst of the USA (eds. Palmer AN, Palmer M). National Speleological Society. pp 332–337
38. Miller T, Brocard G, Willenbring JK (2017) A chronology of karstification In Puerto Rico using cosmogenic dating of cave sediments. Proceedings of the 17th Int Cong Speleol 17
39. Miller TE (2018) Karst notes from the stricken land: Hurricane Maria and the Camuy Caverns. NSS News 76:4–8
40. Moyer RP, Bauer JE, Grottoli AG (2013) Carbon isotope biogeochemistry of tropical small mountainous river, estuarine, and coastal systems of Puerto Rico. Biogeochem 112:589–612. http://doi10.1007/s10533-012-9751-y
41. Nichols G (2009) Sedimentology and Stratigraphy. 2nd ed., John Wiley & Sons. https://doi.org/10.1007/s10533-012-9751-y
42. Ortiz M, Legatzki A, Neilson JW, Fryslie B, Nelson WM, Wing RA, Soderlund CA, Pryor BM, Maier RM (2014) Making a living while starving in the dark: Metagenomic insights into the energy dynamics of a carbonate cave. ISME J 8:478–491. https://doi.org/10.1038/ismej.2013.159

43. Padilla I, Irizarry C, Steele K (2011) Historical contamination of groundwater resources in the north coast aquifers of Puerto Rico. Rev Dimension 3:7–12
44. Padilla IY, Vesper DJ (2018) Fate, transport, and exposure of emerging and legacy contaminants in karst systems: state of knowledge and uncertainty. In Karst Groundwater Contamination and Public Health (eds. White WB, Herman JS, Herman EK) Advances in Karst Science. Springer International Publishing. pp 33–49. https://doi.org/0.1007/978-3-319-51070-5_5
45. Panno SV, Curry BB, Wang H, Hackley KC, Liu CL, Lundstrom C, Zhou J (2004) Climate change in southern Illinois, USA, based on the age and δ13C of organic matter in cave sediments. Quat 61:301–313. https://doi.org/10.1016/j.yqres.2004.01.003
46. Pasch RJ, Penny AB, Berg R (2017) National Hurricane Center Tropical Cyclone Report: Hurricane Maria. National Oceanic and Atmospheric Administration. AL 152017. ftp://ftp.nhc.noaa.gov/atcf
47. Pipan T, Culver DC (2013) Organic carbon in shallow subterranean habitats. Acta Carsologica 42:291–300. https://doi.org/10.3986/ac.v42i2.603
48. Polk JS, van Beynen P, Asmerom Y, Polyak VJ (2013) Reconstructing past climates using carbon isotopes from fulvic acids in cave sediments. Chem Geol 360–361:1–9. https://doi.org/10.1016/j.chemgeo.2013.09.022
49. Rice JA, MacCarthy P (1991) Statistical evaluation of the elemental composition of humic substances. Organ Geochem 17:635–648. https://doi.org/10.1016/0146-6380(91)90006-6
50. Rossel PE, Vähätalo AV, Witt M, Dittmar T (2013) Molecular composition of dissolved organic matter from a wetland plant (Juncus effusus) after photochemical and microbial decomposition (1.25 year): Common features with deep sea dissolved organic matter. Organ Geochem 60:62–71. https://doi.org/10.1016/j.orggeochem.2013.04.013
51. Rowe H, Hughes N, Robinson K (2012) The quantification and application of handheld energy-dispersive x-ray fluorescence (ED-XRF) in mudrock chemostratigraphy and geochemistry. Chem Geol 324–325:122–131. https://doi.org/10.1016/j.chemgeo.2011.12.023
52. Sayer EJ, Lopez-Sangil L, Crawford JA, Bréchet LM, Birkett AJ, Baxendale C, Castro B, Rodtassana C, Garnett MH, Weiss L, Schmidt MWI (2019) Tropical forest soil carbon stocks do not increase despite 15 years of doubled litter inputs. Sci Rep 9. https://doi.org/10.1038/s41598-019-54487-2
53. Schlüter S, Henjes S, Zawallich J, Bergaust L, Horn M, Ippisch O, Vogel HJ, Dörsch P (2018) Denitrification in soil aggregate analogues-effect of aggregate size and oxygen diffusion. Front Environ Sci 6. https://doi.org/10.3389/fenvs.2018.00017
54. Schmidt MW, Torn MS, Abiven S, Dittmar T, Guggenberger G, Janssens IA, Kleber M, Kogel-Knabner I, Lehmann J, Manning DA, Nannipieri P, Rasse DP, Weiner S, Trumbore SE (2011) Persistence of soil organic matter as an ecosystem property. Nature 478:49–56. https://doi.org/10.1038/nature10386
55. Schwarzenbach RP, Gshwend PM, Imboden DM (2016) Environmental Organic Chemistry, 3rd Edition, John Wiley and Sons, Inc. https://doi.org/10.1080/03067319.2017.1318869
56. Simon KS (2019) Chap. 26 - Cave ecosystems. In Encyclopedia of Caves (Third Edition) (eds. White WB, Culver DC, Pipan T). Academic Press. pp 223–226. https://doi.org/10.1016/B978-0-12-814124-3.00025-X
57. Simon KS, Benfield EF, Macko SA (2003) Food web structure and the role of epilithic biofilms in cave streams. Ecology 84:2395–2406. https://doi.org/10.1890/02-334

58. Simon KS, Pipan T, Culver DC (2007) A conceptual model of the flow and distribution of organic carbon in caves.J Cave Karst Stud69. https://digital.lib.usf.edu/SFS0063159/00001
59. Torres NI, Rivera VL, Padilla IY, Macchiavelli RE, Kaeli D, Alshawabkeh AN (2019) Effect of hydrogeological and anthropogenic factors on the spatial and temporal distribution of CVOCs in the karst system of northern Puerto Rico. Environ Earth Sci 78. https://doi.org/10.1007/s12665-019-8611-7
60. Torres NI, Yu X, Padilla IY, Macchiavelli RE, Ghasemizadeh R, Kaeli D, Cordero JF, Meeker JD, Alshawabkeh AN (2018) The influence of hydrogeological and anthropogenic variables on phthalate contamination in eogenetic karst groundwater systems. Environ Pollut 237:298–307. https://doi.org/10.1016/j.envpol.2018.01.106
61. van Hengstum PJ, Reinhardt EG, Beddows PA, Gabriel JJ (2010) Linkages between Holocene paleoclimate and paleohydrogeology preserved in a Yucatan underwater cave. Quat Sci Rev 29:2788–2798. https://doi.org/10.1016/j.quascirev.2010.06.034
62. Vesper DJ, White WB (2003) Metal transport to karst springs during storm flow: an example from Fort Campbell, Kentucky/Tennessee, USA. Hydrol J 276:20–36. https://doi.org/10.1016/s0022-1694(03)00023-4
63. Vesper DJ, White WB (2004) Spring and conduit sediments as storage reservoirs for heavy metals in karst aquifers. Environ Geol 45:481–493. https://doi.org/10.1007/s00254-003-0899-6
64. von Fischer JC, Tieszen LL (1995) Carbon isotope characterization of vegetation and soil organic matter in subtropical forests in Luquillo, Puerto Rico. Biotropica 27:138–148. https://doi.org/10.2307/2388989
65. Wanzek T, Keiluweit M, Varga T, Lindsley A, Nico PS, Fendorf S, Kleber M (2018) The ability of soil pore network metrics to predict redox dynamics is scale dependent. Soil Syst 2. https://doi.org/10.3390/soilsystems2040066
66. White W (2007) Cave sediments and paleoclimate. J Cave Karst Stud 69:76–93
67. White WB (1988) Geomorphology and Hydrogeology of Karst Terrains. Oxford University Press
68. Yu X, Ghasemizadeh R, Padilla I, Irizarry C, Kaeli D, Alshawabkeh A (2015) Spatiotemporal changes of CVOC concentrations in karst aquifers: analysis of three decades of data from Puerto Rico. Sci Total Environ 511:1–10. https://doi.org/10.1016/j.scitotenv.2014.12.031
69. Yu X, Ghasemizadeh R, Padilla I, Irizarry C, Kaeli D, Alshawabkeh A (2015) Spatiotemporal changes of CVOC concentrations in karst aquifers: analysis of three decades of data from Puerto Rico. Sci Total Environ 511:1–10. https://doi.org/10.1016/j.scitotenv.2014.12.031

# Figures

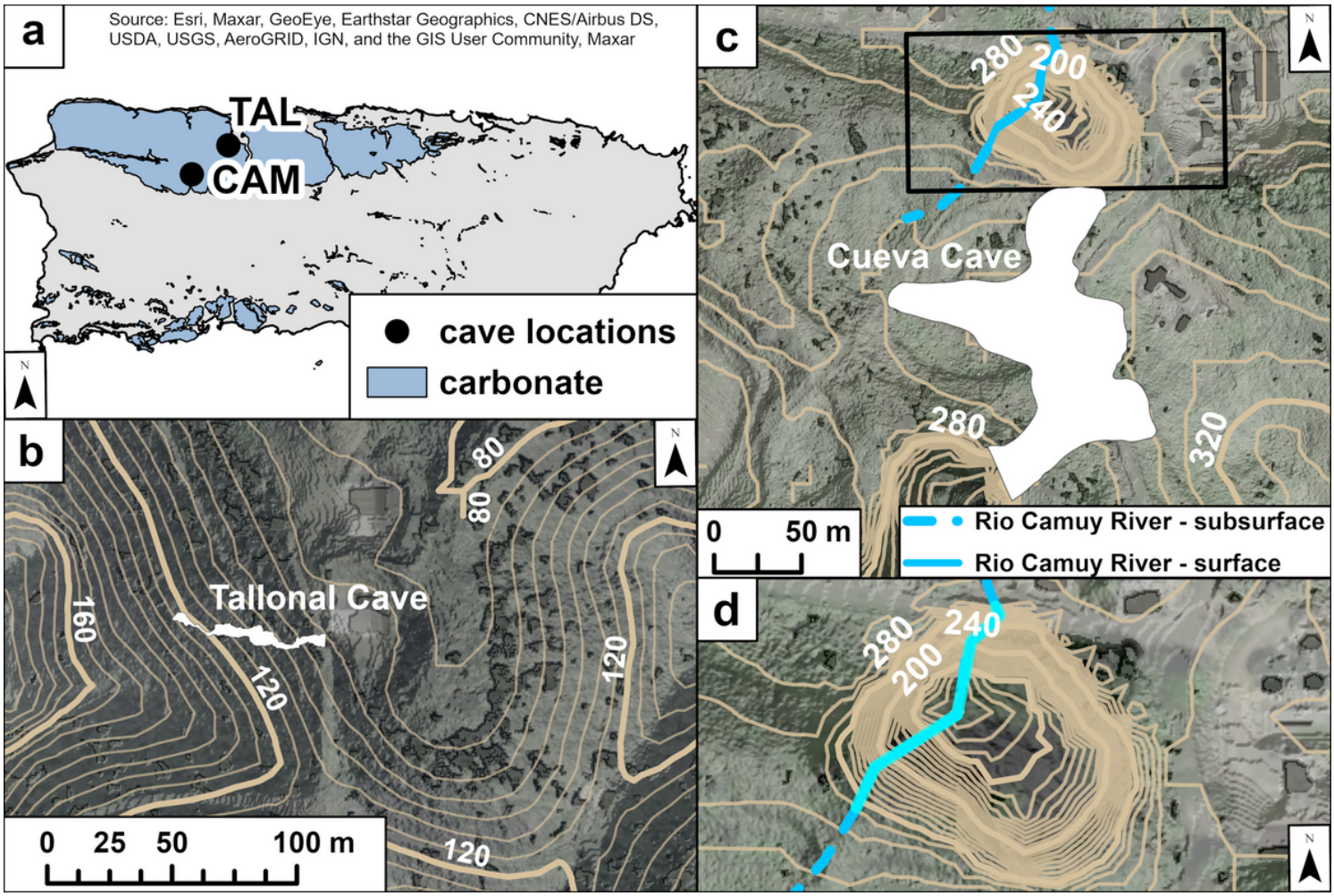


**Figure 1**

(a) Puerto Rico's major carbonate-karst areas with the locations of the two caves included in this study. (b) Aerial imagery and regional topography surrounding El Tallonal Cave (TAL) with the plan view of TAL included. (c) Aerial imagery and topography surrounding Cueva Cave (CAM) with the plan view of CAM included. (d) Aerial imagery of the northern sinkhole in map c (extent indicated in map c) with the approximate flow path of the Río Camuy River. Dashed line represents subsurface flow of the Río Camuy River

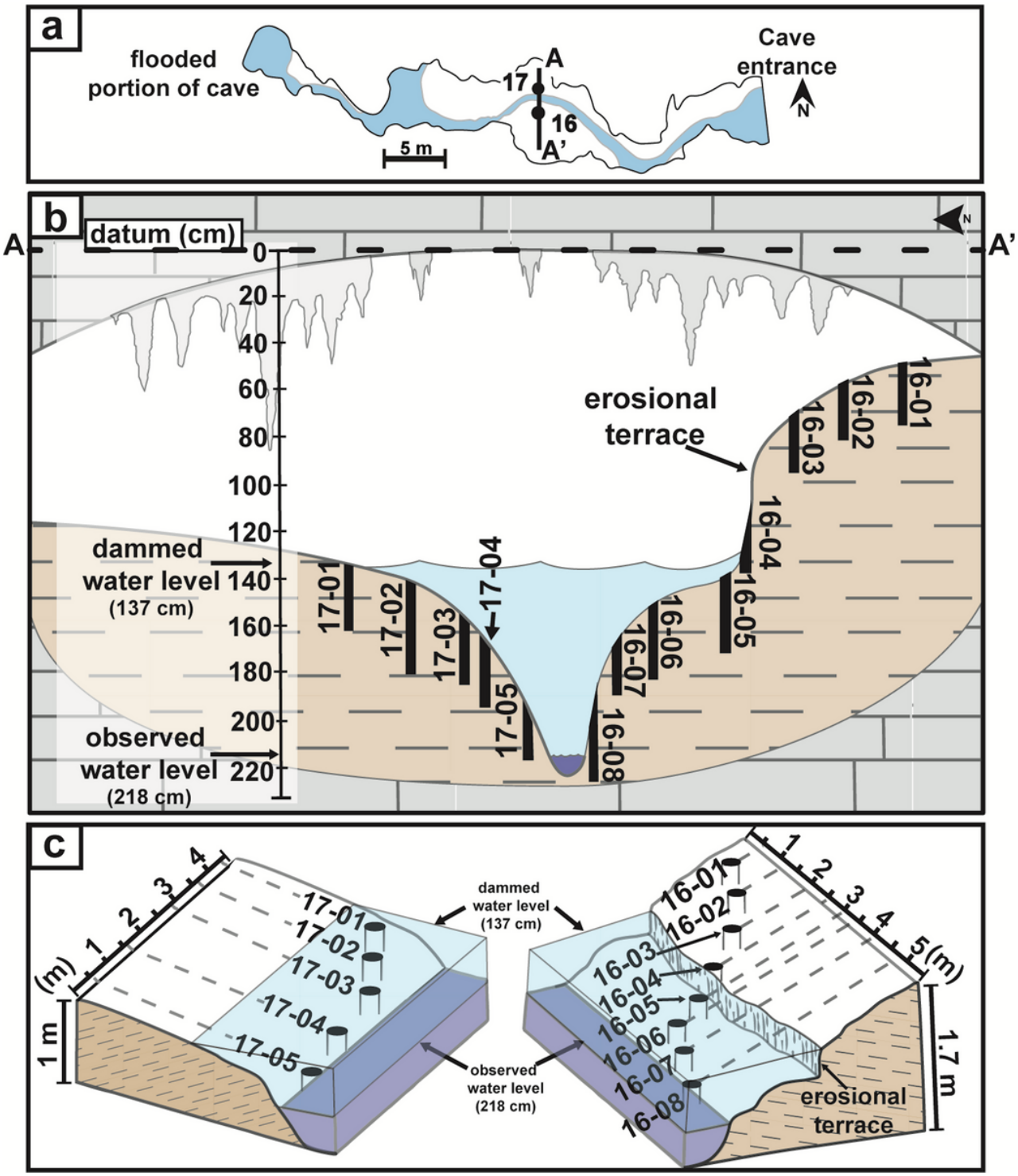


## Figure 2

Sample locations in TAL (Tallonal Cave). (a) Plan view of the entire cave passage with sample locations 16 and 17 indicated along with a cross sectional line from A-A'. Flow is eastward from the flooded portion toward the cave entrance. (b) Generalized cross section from A-A' with sample locations included. Labeled samples are individual cores. Samples were given a depth relative to the datum illustrated on this figure. Observed water level (darker blue) and dammed water level (lighter blue) are at 218 cm and 137 cm respectively. (c) The spatial distribution of sample locations 16 and 17. Sediment cores were collected in a diagonal transect along both sediment banks. Only the observed water level is shown in c

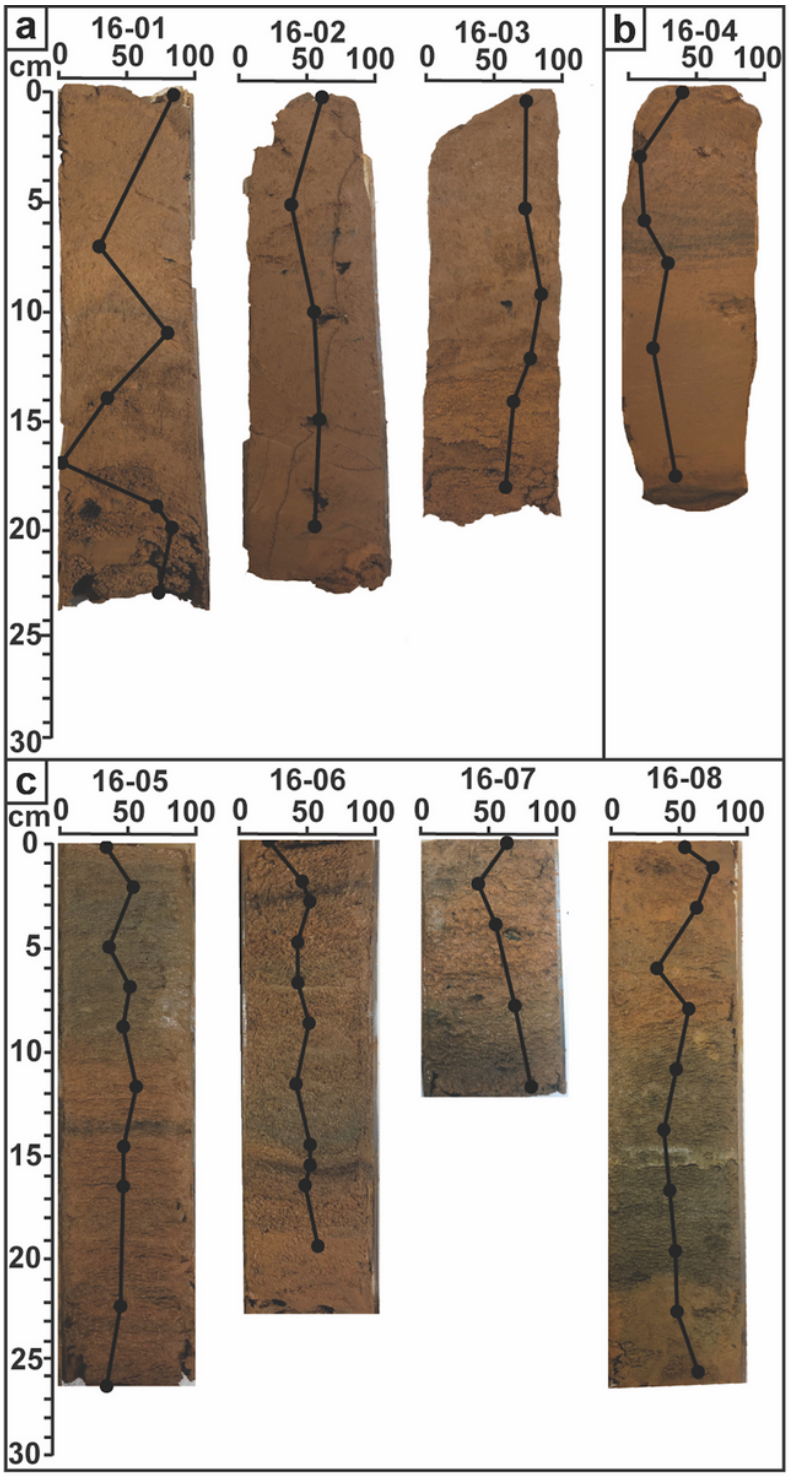


## Figure 3

(a) Unsaturated sediment cores, (b) core 16-04, (c) and saturated sediment core photographs collected from location 16 with the proportion of sand superimposed. Core 16-01 is the top of the sediment bank and 16-04 was collected from the erosional terrace. Note the redox banding in 16-04 (b) and the saturated samples (c)

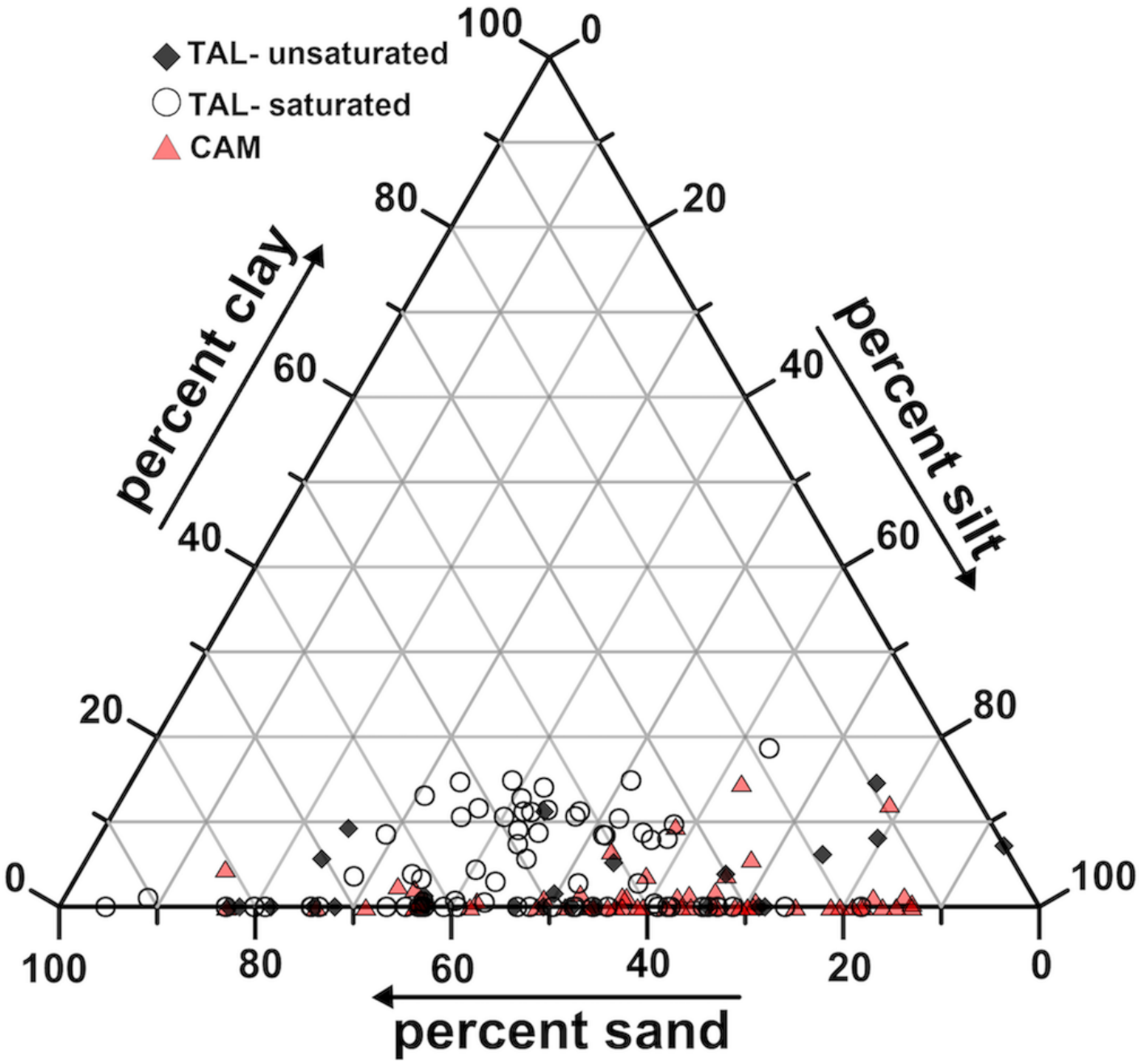


**Figure 4**

Grain size distribution of samples collected from TAL and CAM. Unsaturated and saturated samples from TAL are indicated

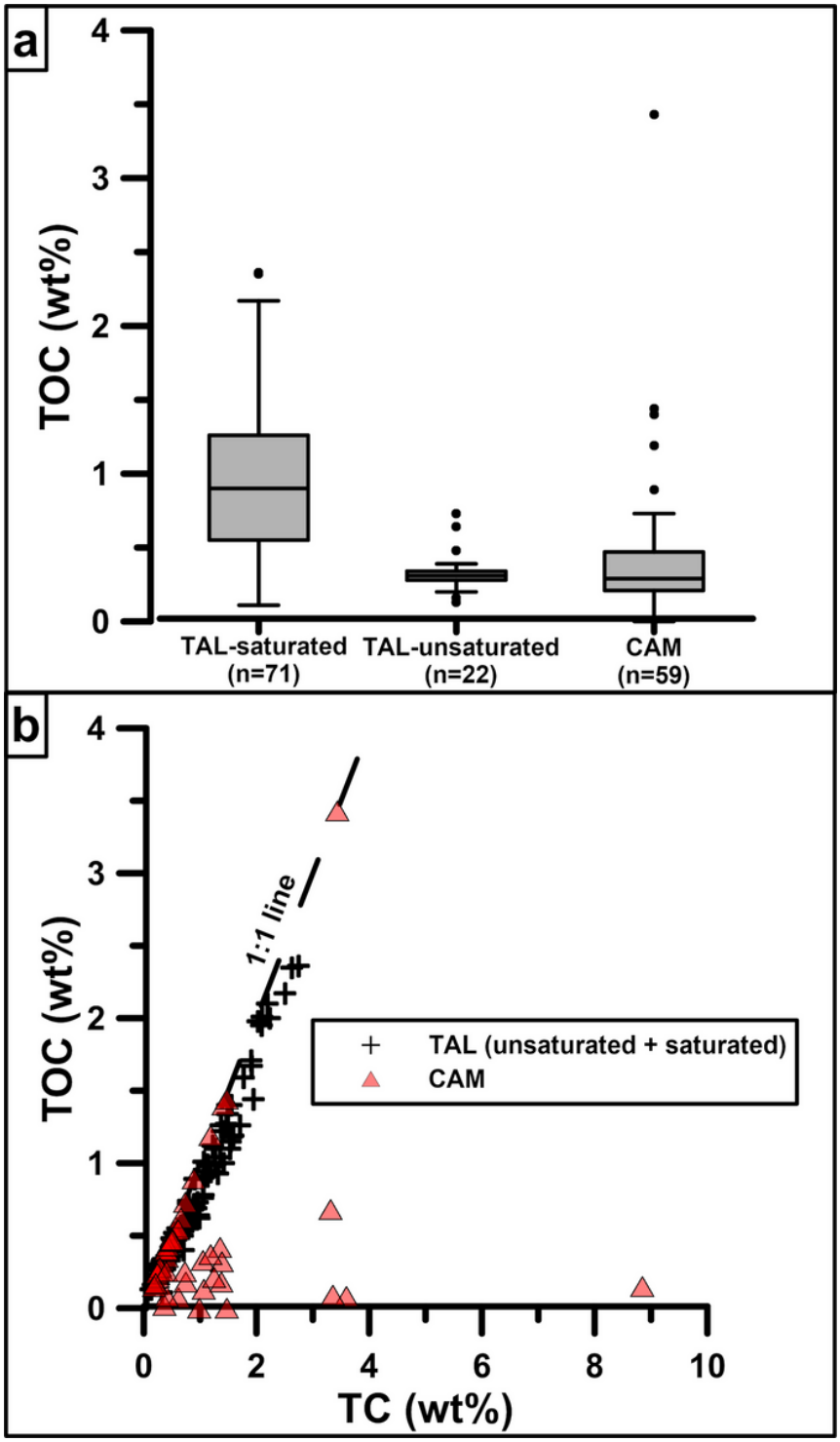


**Figure 5**

(a) Range of total organic carbon (TOC) in saturated and unsaturated samples from TAL and CAM. Outliers are plotted for each data set. (b) Total carbon (TC) versus total organic carbon (TOC) of sediment samples from TAL and CAM. Both saturated and unsaturated sediments from TAL are plotted together

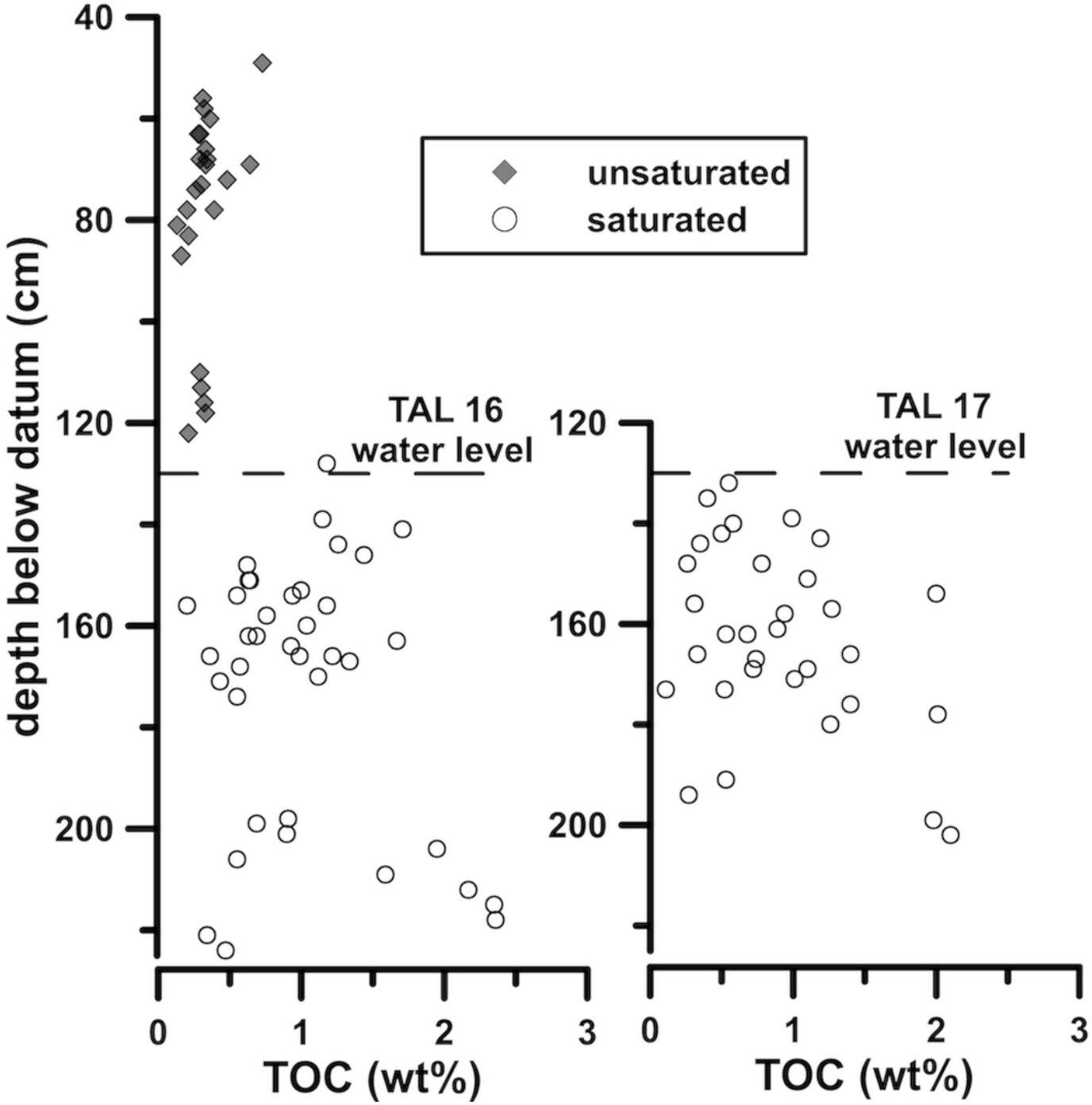


**Figure 6**

Total organic carbon (TOC; wt%) of sediment samples collected from cores 16 and 17 at TAL. Samples are plotted relative to the datum. The water level for location 16 and 17 is at an elevation of 137 cm relative to the datum (dashed line)

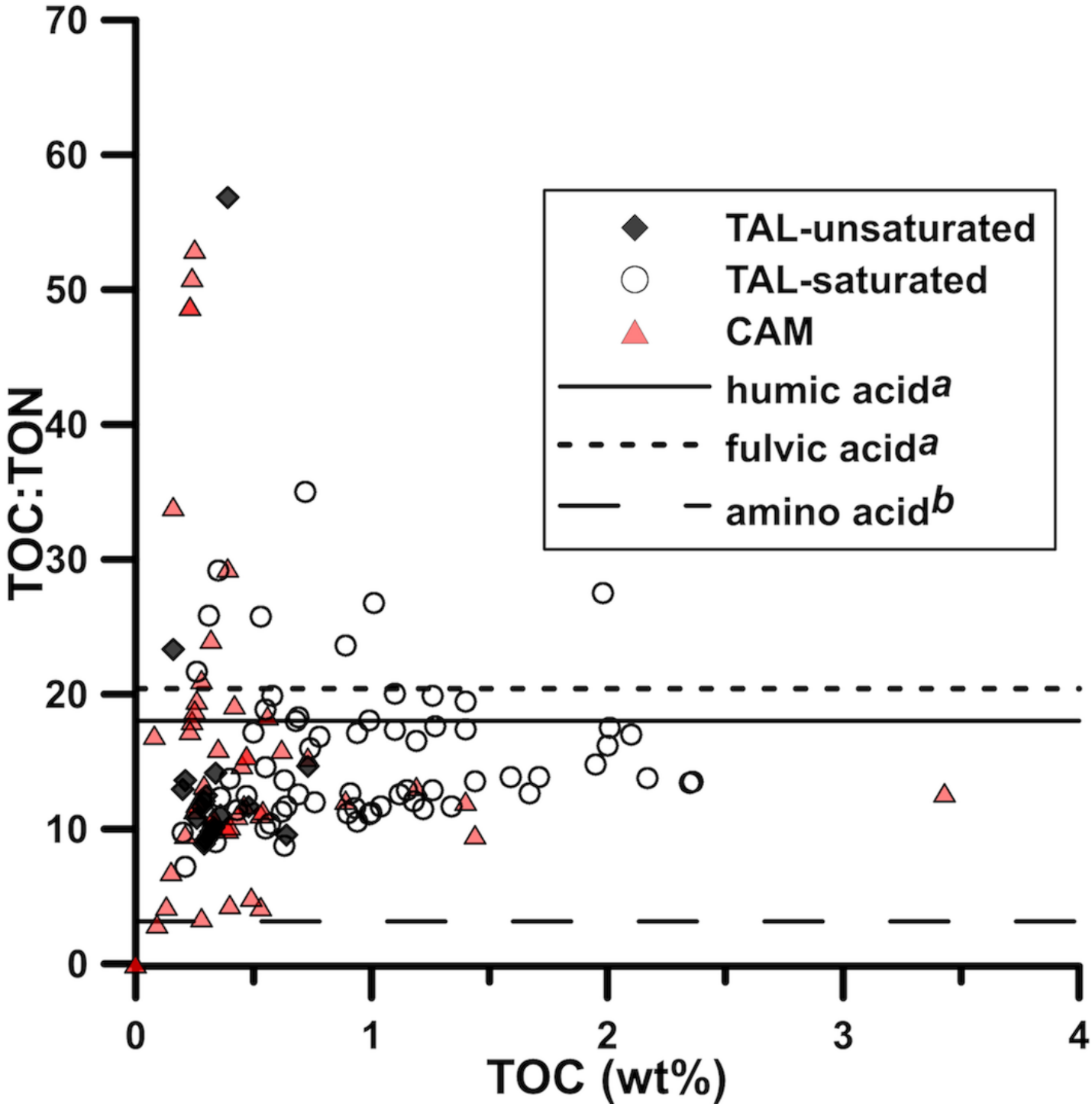


**Figure 7**

Total organic carbon (TOC) versus the ratio of total organic carbon to total organic nitrogen (TOC:TON). Carbon nitrogen ratios (C:N) of humic acid, fulvic acid, and amino acids are listed for comparison. Average fulvic acid (20.4, range 7.0-147), humic acid (average 18.0, range 6.2-75.1), and amino acid (3.2 range 2.9-3.6) C:N values are represented by horizontal lines: a Rice and MacCarthy (1991), b Jover et al. (2014)

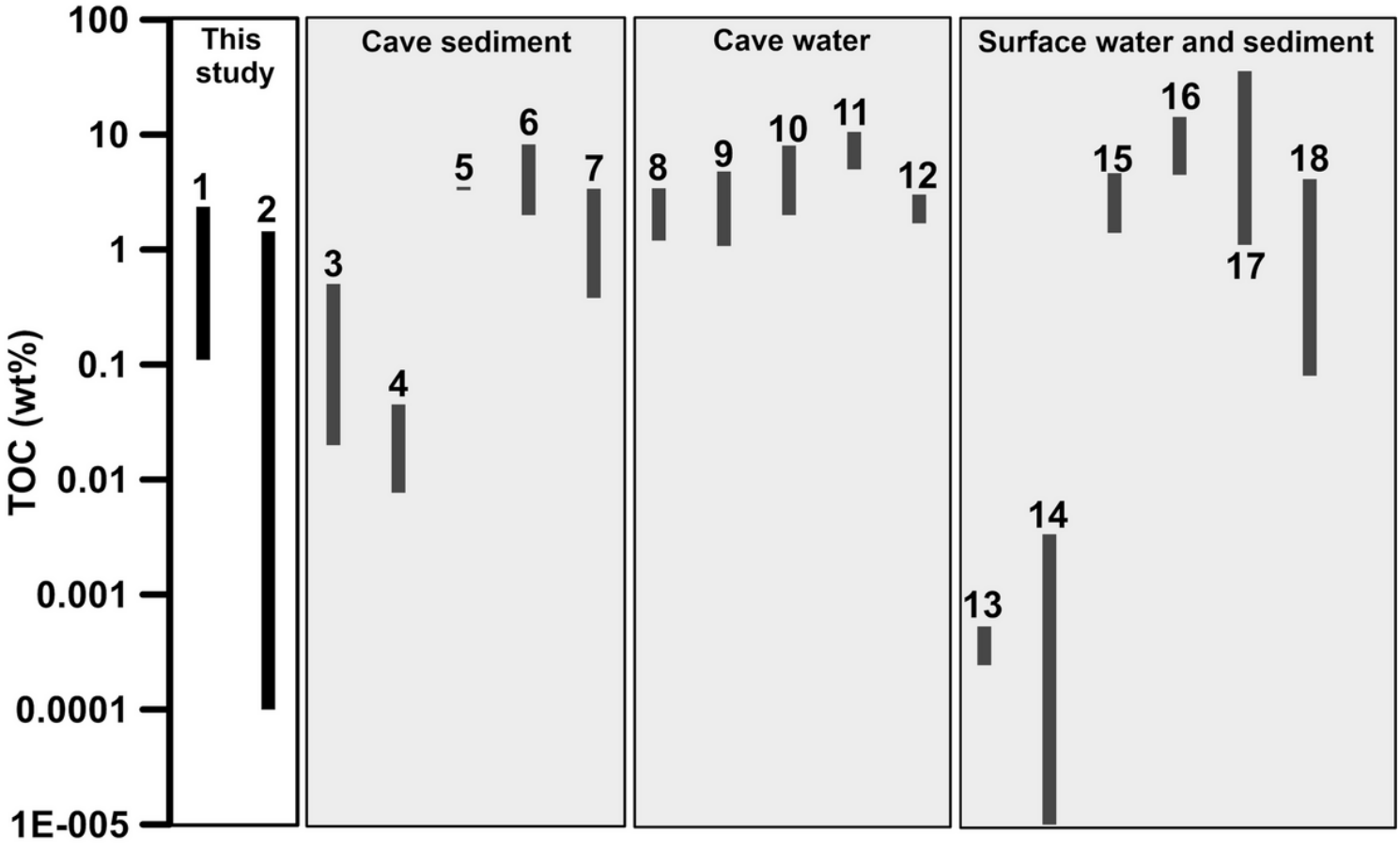


**Figure 8**

Comparison of TOC concentrations from cave streams and clastic cave sediment (boxed) and surface sediments (unboxed) from various geographic locations. Plotted data sets are numbered according to the references listed in Table 1

## Supplementary Files

This is a list of supplementary files associated with this preprint. Click to download.

- S1.tif
- S2.tif
- S3Data.xlsx